JOURNAL OF CATALYSIS **176,** 459–473 (1996)
ARTICLE NO. CA982065

# Partial Oxidation of $C_5$ and $C_6$ Alkanes over Monolith Catalysts at Short Contact Times[1]

A. G. Dietz III, A. F. Carlsson, and L. D. Schmidt[2]

*Department of Chemical Engineering and Materials Science, University of Minnesota, Minneapolis, Minnesota 55455*

Received July 22, 1997; revised February 27, 1998; accepted March 2, 1998

**Olefins can be produced with high selectivity and yield by oxidative dehydrogenation of $C_2$ to $C_4$ alkanes autothermally over Pt coated foam monolith catalysts at contact times of ~5 ms at atmospheric pressure and 700–900°C. In this paper we extend these reactions to higher alkanes by reacting pentane, isopentane, n-hexane, or cyclohexane vapor mixed with air or $O_2$ in a nearly adiabatic tubular reactor consisting of an $\alpha$-$Al_2O_3$ foam monolith catalyst coated with a Pt film. Pentane and n-hexane form primarily ethylene and propylene at low fuel/$O_2$ ratios and form primarily $C_5$ and $C_6$ linear olefins at high fuel/$O_2$ ratios. Isopentane produces primarily isobutylene over a wide range of fuel/$O_2$ ratios and never favors production of isopentene. Cyclohexane ring opening reactions dominate at low fuel/$O_2$ ratios with ethylene and 1,3-butadiene production favored, while dehydrogenation reactions occur at high fuel/$O_2$ ratios with cyclohexene, cyclohexadiene, and benzene becoming the dominant products. In contrast to the $C_2$ to $C_4$ alkanes, some oxygen breakthrough is seen at all operating conditions for higher alkanes, and breakthrough can be reduced only slightly by preheating the feed gases. Quenching downstream gases increases $O_2$ and fuel breakthrough somewhat, indicating that some reactions with unreacted $O_2$ are continuing homogeneously downstream of the catalyst. A comparison of alkane oxidation over monolith catalysts with thermal pyrolysis of alkanes shows similar product distribution (ignoring CO and $CO_2$ production), especially at lower fuel/$O_2$ ratios. $\beta$-elimination of H atoms from adsorbed surface species can also explain the distribution of products for the different fuels, and surface reactions explain dehydrogenated products and 1-olefins at high fuel/$O_2$ ratios.** 

## INTRODUCTION

Production of olefins by thermal cracking of hydrocarbons is a major route to many chemical feedstocks (1–4). These pyrolysis reactions take place in long tubular reactors heated to high temperatures to achieve near equilibrium products. Since the process is limited by equilibrium constraints, the reactors and reactions have been modeled extensively so that yields to desired products could be maximized (1, 5–9). Because steam is usually added to the feed gases to reduce formation of solid carbon in the reactor tubes, this process is commonly referred to as steam cracking.

We have found that olefins can also be produced with selectivities up to 70% and alkane conversion up to 80% by partial oxidation over monolithic catalysts at very short contact times (10–12). Ethylene can be produced by ethane oxidation over Pt coated foam monoliths at contact times of ~5 ms with no coke formation and no deactivation after many hours of operation and startup/shutdown cycling. Likewise, isobutylene can be selectively produced by the catalytic oxidation of isobutane over Pt monoliths (12).

Production of olefins with monolith catalysts offers considerable benefits over thermal pyrolysis. Since the monolithic reactors operate autothermally, energy consumption in this process is considerably less than in a steam cracking pyrolysis furnace. Another advantage of monolithic reactors is that they would be ~100 times smaller than their steam cracking counterparts since residence times are much lower in the monolith (5 ms vs 1 s). Furthermore, no evidence of carbon formation is seen on the Pt monolith catalysts or in the reactor after many hours and at pressures up to 6 atm (10, 13).

Previous work over monolith catalysts has shown that linear $C_2$–$C_4$ alkane feeds give linear olefins, and isobutane selectively produces isobutylene (11, 12, 14). With this in mind, we investigated the differences between pentane and isopentane oxidation. Since isobutylene can be selectively produced from isobutane, isopentene production could be possible and could provide a new intermediate step for tert-amyl methyl ether (TAME) synthesis. Production of any cyclo-$C_6$ oxygenated products such as cyclohexanol or cyclohexanone directly from cyclohexane would be valuable, as would a highly selective process to cyclohexene. In addition, the differences in surface chemistry between n-hexane and cyclohexane would provide insight into mechanisms on the catalyst surface and in the gas phase above the surface.

This paper examines the oxidation of pentane, isopentane, hexane, and cyclohexane over monolith catalysts. The focus of the experiments was to determine reaction

[1] This research was supported by DOE under Grant No. DE-FG02-88ER13878 and by CR&L, Pasadena, TX.

[2] To whom correspondence should be addressed.



0021-9517/98 $18.00

conditions in which olefin production is maximized and to understand the chemistries occurring both catalytically and homogeneously. Most of the results are from Pt coated monoliths since they are more selective to olefins, although, some results from Rh coated monoliths are shown for comparison.

*Reactions and Thermodynamics*

Production of $CO_2$, $H_2O$, and CO liberates a large amount of heat which heats the gases very rapidly to >900°C and allows dehydrogenation and cracking reactions to occur. In thermal pyrolysis and steam cracking reactors, cracking reactions occur homogeneously after high temperatures (~800°C) have been achieved, and maximum product yields near thermodynamic equilibrium are achieved at residence times of 0.1 to 1 s. Over monolith reactors any exothermic reactions must occur heterogeneously within 5 ms, after which the gases begin to cool.

Carbon formation inside pyrolysis tubes can result in operating problems and even complete tube blockage (15–19). The coke can form in high-temperature regions of tube furnaces due to reactions of gas phase radicals with the growing solid carbon. It can also form on cool wall sections when high boiling point components condense. For these reasons, steam is added to the feed to prevent coke from forming by reforming the carbon to $CO_2$ and $H_2$.

## EXPERIMENTAL

The reactor was similar to those described previously for synthesis gas production by direct oxidation of methane (20, 21) and for alkane oxidative dehydrogenation to olefins (10). A 17-mm diameter, 10-mm long, metal-coated $\alpha$-$Al_2O_3$ foam monolithic support placed between two extruded cordierite monolith heat shields was fitted inside a 40-cm long quartz tubular reactor. The catalyst and heat shields were wrapped in Fiberfrax alumina cloth to insulate the catalyst, to hold it in place, and to prevent bypass of reactant gases.

Alumina supported catalysts were prepared by coating $\alpha$-$Al_2O_3$ 45 ppi foam monoliths with saturated solutions of the appropriate metal as described previously (20–23) giving typical loadings between 4–6% by weight. The surface area of the alumina was less than 1 $m^2$/g, so that at these loadings the metals formed films on the alumina. Monolith samples remained stable over many days of operation and through several startups and shutdowns. Table 1 summarizes some of the catalyst properties, and average catalyst turnover frequencies (TOF) for these experiments. Since we are using film catalysts, we assume Pt surface area does not change appreciably above 0.5 wt% loading (which corresponds to one monolayer of Pt). Therefore, in the discussion below, TOF will compare directly to fuel and oxygen conversions.

**TABLE 1**

**Typical Monolith Properties**

| | | |
|---|---|---|
| Composition | 3–7 wt% Pt[a] 93–97 wt% $Al_2O_3$ | |
| Channel diameter ($\mu$m) | 444 | |
| Porosity | 80% | |
| Thermal conductivity (W/mK) | 8–11 | |
| Surface area ($cm^2$/g) | 70 | |
| Average turnover frequency ($s^{-1}$) | $O_2$ | Fuel |
| Isopentane–air | 740 | 440 |
| Pentane–air | 660 | 330 |
| Hexane–air | 730 | 350 |
| Cyclohexane–air | 800 | 480 |

[a] Several monolith catalysts with metal loadings of 3–7 wt% Pt were used for these experiments. No effects of metal loadings was observed at these conditions.

Reactant gases (air, $O_2$, and $N_2$) were introduced from high pressure cylinders through mass flow controllers. To maintain metered flow of gaseous fuel without any fluctuations, a liquid vaporization apparatus was designed and built. A syringe pump was used to introduce liquid hydrocarbon fuels. The liquid evaporated in a coiled 1/8 in. diameter stainless steel tube placed in a fluidized bed heater. The vapor was then passed through a superheater packed with stainless steel filings and through a pressure regulator which maintained pressures in the superheater and fluidized bed at 20 psig. Typical gas flowrates through the reactor were 5 slpm, corresponding to 200–400 ml/hour of liquid. Pulsing due to variation in the evaporation rate of the liquid was observed immediately after the fuel flow was started, but this subsided within a few minutes. Observation of pulsing during experimental runs could best be observed by monitoring any fluctuations in catalyst temperature after steady state was achieved, since any change in fuel flow would greatly affect catalyst operation. No temperature changes due to pulsing were detected during operation.

The vaporized fuel was then mixed with the remaining reactant gases and fed directly into the reactor through heated stainless steel lines. The air, $O_2$, and $N_2$ lines were also preheated to prevent any fuel condensation at the fuel/air mixing point. The reactant gases upstream of the catalyst were maintained at a specified temperature with a heating tape connected to a temperature controller. Pressure in the reactor and gas chromatograph sample lines was maintained at 3 psig with a downstream valve so that a fraction of the gases could be sent to a gas chromatograph for analysis. Temperatures of the fuel and mixed gases were observed at several points with chromel–alumel thermocouple probes, and temperature at the downstream catalyst surface was monitored with a Pt–Rh thermocouple. All product gases were incinerated with a Bunsen burner.

*Safety and Flammability*

Proper and constant vaporization of the liquid fuel is necessary to ensure safe operation of the reactor. Since operation requires air and fuel mixtures close to the homogeneous flammability limits, any variation due to pulsing of the fuel could be disastrous, especially when fuel and air mixtures are passing over a hot catalytic surface. In early attempts to vaporize the liquids, pulsing of the liquid caused flames upstream of the catalyst which propagated back to the fuel/air mixing point. As a result, carbon was deposited in the reactor, and the catalyst was ruined due to carbon formation and high temperatures.

Much care was taken to ensure constant fuel delivery. We attempted to maximize heat transfer to the fuel in the fluidized bed heater, minimize condensation by superheating the fuel, damp any pulsing with a back pressure regulator, and fit the system with multiple check valves, relief valves, and rupture disks. Even with these precautions, it was essential to avoid any irregularities because even a small disturbance could cause a flame or explosion.

*Startup and Shutdown*

The reactor was operated autothermally in that the heat generated by the reactions is large enough to maintain reaction on the catalyst after ignition. To light off the catalysts, the fuel flow was first allowed to stabilize before any oxidant was introduced. Next, the air or oxygen flow was increased until the appropriate fuel/oxygen ratio was achieved (typically 0.8). The reactant gases were then preheated to approximately 210°C with heating tape, after which the catalyst ignited. Gas flows were then set to desired conditions. The reaction attained steady state operating conditions within 15 min of ignition, and no significant transients or deactivation were observed in these experiments over periods of many hours.

Since the feed gas ratios were on the fuel-rich side of the flammability limits, the reaction was shut down by turning off the air or $O_2$ first, and then turning off the fuel flow.

*Product Analysis*

Product gases were analyzed with a HP6890 gas chromatograph equipped with a narrow bore (320 $\mu$m) Poropak Q capillary column. Argon carrier gas was used to quantify hydrogen production, while helium carrier gas was used to quantify the remaining products. Nitrogen was the calibration gas for mass balances since it is inert in these processes. The amount of water formed in the reaction was calculated from oxygen atom balances due to fluctuation of the size of this peak. Flow rates through the mass flow controllers were accurate to within $\pm 0.05$ slpm, carbon and hydrogen atom balances closed to within $\pm 6\%$ (usually $\pm 3\%$), and individual species concentrations were measured with a reproducibility of $\pm 1\%$.

## RESULTS

The majority of experiments were performed over several Pt coated $Al_2O_3$ monoliths with 3–7 wt% Pt, while data from a single 3 wt% Rh-coated monolith is included for comparison. We begin with results from n-pentane and n-hexane oxidation, then isopentane, and conclude with cyclohexane oxidation. All measured reaction temperatures at the exit of the monoliths for these systems were within 50°C of the calculated adiabatic reaction temperatures.

Conversions ($\Delta F_{fuel}/F_{fuel,\,in}$) and selectivities ($\nu \cdot F_{product,\,out}/\Delta F_{fuel}$, where F represents flow rate and $\nu$ is the stoichiometric factor) were determined from the molar flows into and exiting the reactor as described earlier (11, 20, 23). Product yield is defined as the product of conversion and selectivity, all on a molar basis.

*Pentane*

Figure 1 shows product carbon atom selectivities, reactant conversions, and reaction temperature for pentane oxidation in air over a Pt monolith as a function of $C_5H_{12}/O_2$ ratio in the feed gas. The reactants were fed at a constant mass flowrate of 5 standard liters per minute which corresponds to a gas hourly space velocity of $1.56 \times 10^5$ $h^{-1}$. If a constant temperature is assumed across the catalyst, this velocity corresponds to an average residence time of $6.5 \times 10^{-3}$ s (P = 1.2 atm, T = 900°C).

Figure 1 shows that as $C_5H_{12}/O_2$ ratio increases and $C_5H_{12}$ conversion decreases, conversion of $O_2$ changes from 0.88 to 0.70, and then sharply decreases to 0.47. This represents considerable oxygen breakthrough, which is not seen when reacting $C_1$–$C_4$ alkanes over Pt monoliths. Reaction was sustained at the higher $C_5H_{12}/O_2$ ratios for several hours and did not extinguish.

Two regions of operation are evident in pentane oxidation. From a $C_5H_{12}/O_2$ ratio of 0.5 to 0.9, olefin production dominates, and CO is produced rather than $CO_2$. At $C_5H_{12}/O_2$ ratio of 1.0, fuel and $O_2$ conversion and olefin selectivity drop quickly, $CO_2$ and $H_2O$ production is favored, and acetaldehyde selectivity increases by a factor of 3. In the olefin production regime, ethylene, propylene, and 1-butene are formed, and the molar ratios of $C_2H_4 : CH_4 : C_3H_6 : C_4H_8$ range from 20 : 10 : 6 : 1 to 6 : 3 : 3 : 1. In the fuel-rich regime, production of $C_5$ olefins begins to dominate.

Figure 2 shows data from pentane oxidation in enriched air (40% $N_2$ diluent). Again, two operating regions are present, except now they are shifted to richer $C_5H_{12}/O_2$ ratios. Compared to pentane/air oxidation, in the "lean" regime, selectivity to olefins is greater, and in the "rich" regime selectivity to oxygenated products is greater. The larger olefin selectivity can be attributed to an increase in selectivity to propylene, which becomes the dominant product at a $C_5H_{12}/O_2$ ratio of 1.6 before it is replaced by the $C_5$ olefins in the "rich" regime.

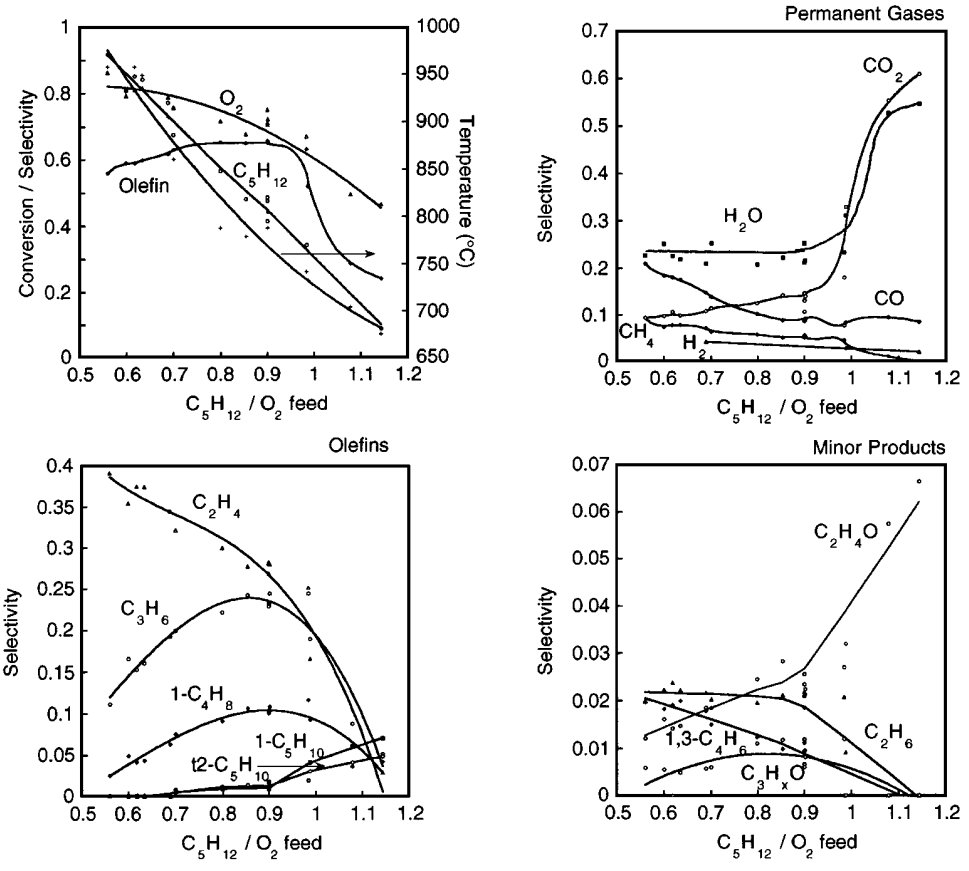


**FIG. 1.** Selectivity and conversion in n-pentane oxidation in air versus $C_5H_{12}/O_2$ over a Pt coated foam monolith (45 ppi). In these experiments, the reactant gases were preheated to 200°C and the flow rate was 5 slpm.

At the richest $C_5H_{12}/O_2$ ratios, $C_5$ olefin production doubles from that in pentane/air oxidation. In addition, selectivity to acetaldehyde doubles, and the production of formaldehyde and $C_3$ oxygenates is evident, while formation of $CO_2$ is 50% less. Water formation is also lower with enriched air.

For all pentane oxidation experiments over Pt monoliths, the dominant olefin products were $C_2H_4$ and $C_3H_6$ in the "lean" regime and singly dehydrogenated $C_5$ olefins in the "rich" regime. No branched olefins were identified (<100 ppm), and 1,3-$C_4H_6$ production was minimal (selectivity of 0.00–0.02). In all cases over Pt, the selectivity to $H_2$ was lower than 0.07.

When a mixture of pentane and air reacted over a Rh coated monolith, the distribution of products was considerably different from pentane oxidation over Pt. Figure 3 shows that as the $C_5H_{12}/O_2$ ratio was raised the conversion of fuel dropped nearly linearly from 0.83 to 0.4 while conversion of $O_2$ was not complete at any fuel/$O_2$ ratio, remaining roughly constant at 0.87. Total olefin selectivity remained relatively constant at around 0.45 over the range of feeds. It is important to note that CO formation was favored at all compositions while $CO_2$ production was suppressed and that $H_2$ selectivities of 0.30 could be achieved at the leanest compositions. Ethylene, propylene, and 1-butene were the major olefins produced with small amounts (<0.02) of 1,3-butadiene also detected. Since the values are reported as carbon atom selectivity, the molar ratio of $C_2H_4 : CH_4 : C_3H_6 : C_4H_8$ ranges from 14 : 7 : 5 : 1 to 4 : 2 : 2 : 1. Roughly equal molar amounts of methane and 1-butene were formed at all $C_5H_{12}/O_2$ ratios.

*Isopentane and n-Hexane*

Results from isopentane and n-hexane oxidation in air over Pt monoliths are shown in Figs. 4 and 5. For each of these fuels, the two regions of operation are evident. It is important to notice that similarly to n-pentane, n-hexane selectively forms cracked olefins at low fuel/$O_2$ ratios and forms n-hexene at high fuel/$O_2$ ratios. However, isopentane forms $C_4$ olefins selectively in both regions, even when production of iso-$C_5$ olefins begins.

Reaction of isopentane produces $C_4$ olefins with the highest selectivity. Isobutylene production dominates, followed by the cis and trans 2-butenes. 2-methyl-1-butene is the dominant $C_5$ olefin product by more than a factor of three. We again see CO formation at low i-$C_5H_{12}/O_2$ ratios and $CO_2$ formation at high i-$C_5H_{12}/O_2$ ratios, but acetaldehyde production is now six times smaller than in pentane oxidation.

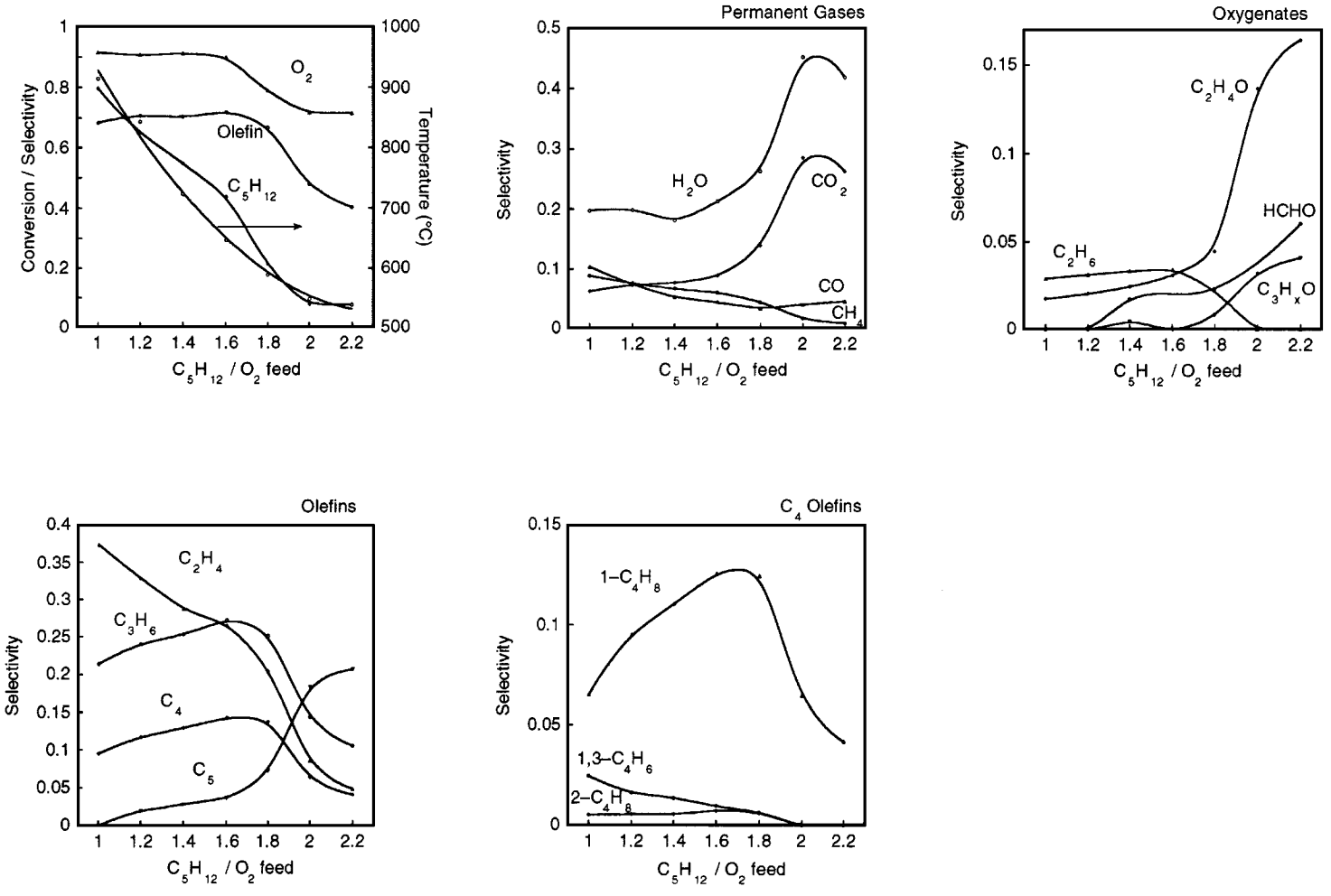


**FIG. 2.** Selectivity and conversion in n-pentane oxidation in enriched air (40% $N_2$ diluent) versus $C_5H_{12}/O_2$ over a Pt coated foam monolith (45 ppi). In these experiments, the reactant gases were preheated to 200°C and the flow rate was 3 slpm.

The data for n-hexane/air oxidation over Pt show similar results to pentane/air oxidation. Cracking products ($C_2H_4$ and $C_3H_6$) are favored at low $C_6H_{14}/O_2$ ratios and the dehydrogenated parent is favored at high $C_6H_{14}/O_2$ ratios. However, at a $C_6H_{14}/O_2$ ratio of 1.15 the selectivity to $C_6$ olefins is 0.32 which is nearly twice $C_5$ olefin selectivity in pentane/enriched air oxidation, three times $C_5$ olefin selectivity in pentane/air oxidation, and four times i-$C_5$ olefin selectivity in i-pentane/air oxidation. The selectivity to 1-hexene is substantially higher than the selectivity to 2-hexene. In addition, some rearranged $C_6$ olefins are produced in small amounts. When fuel and $O_2$ conversion drop at high $C_6H_{14}/O_2$ ratios, water, $CO_2$, and acetaldehyde selectivities all increase. Formation of acetaldehyde is double that in pentane/air oxidation.

*Cyclohexane*

Figure 6 shows results for cyclohexane oxidation in air over a Pt coated foam monolith. Cyclohexane conversion decreases with increasing $C_6H_{12}/O_2$ ratio, but $O_2$ conversion decreases only slightly, remaining above 0.80 at high $C_6H_{12}/O_2$ ratios. Some similar trends to noncyclic alkane oxidation exist, but a definite separation into two operating regimes is not as apparent. Catalyst temperatures range from ~800 to 600°C which is about 100° cooler than for noncyclic alkane oxidation.

Ethylene and $C_4$ olefins are selectively produced at low $C_6H_{12}/O_2$ ratios, while at high $C_6H_{12}/O_2$ ratios, $C_6$ olefins are favored. No straight-chain $C_6$ olefins were detected, only cyclized $C_6$ olefins. Selectivity to cyclohexene can be maintained above 0.25 at high $C_6H_{12}/O_2$ ratios, while benzene and cyclohexadiene are produced in smaller quantities, giving evidence for multiple dehydrogenation of the fuel. For the noncyclic oxidations, multiple dyhydrogenations (1,3-$C_4H_6$) accounted for less than 0.03 in total selectivity.

The dominant $C_4$ olefin product in cyclohexane oxidation is 1,3-butadiene, compared to butenes for the other oxidation reactions. Smaller amounts of butenes are formed from cyclohexane, but butadiene selectivity is more than 10 times greater, and reaches a maximum of 0.15 between $C_6H_{12}/O_2$

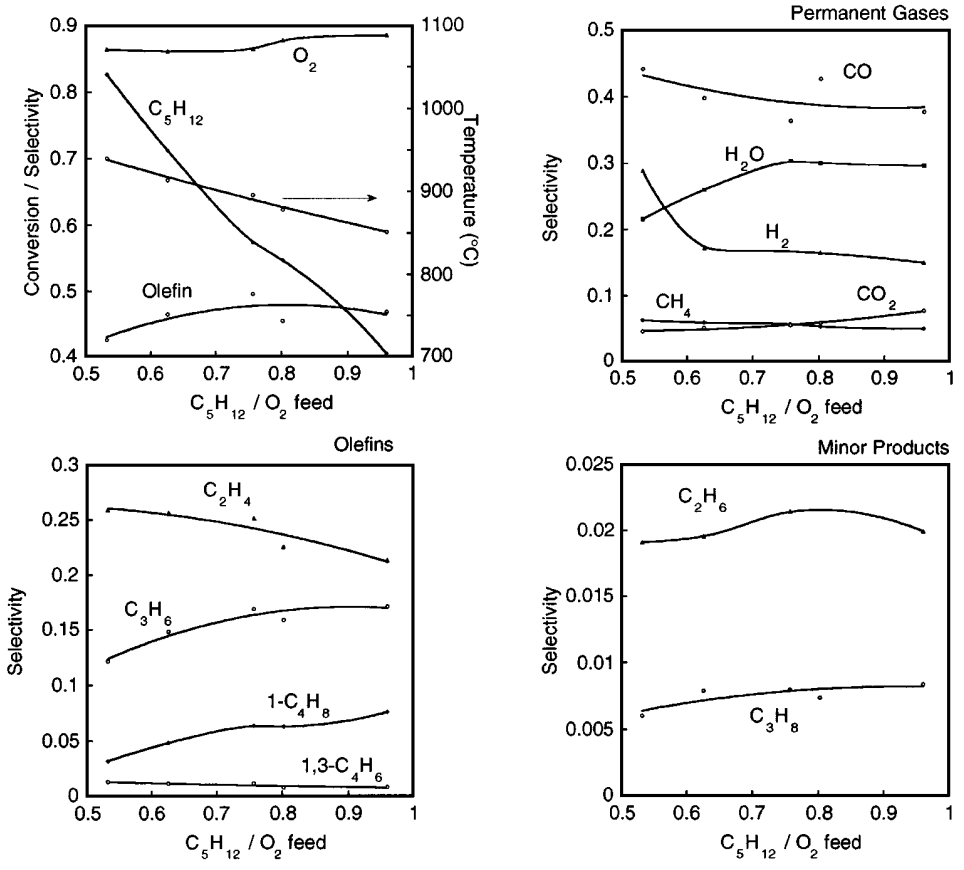


**FIG. 3.** Selectivity and conversion in n-pentane oxidation in air versus $C_5H_{12}/O_2$ over a Rh coated foam monolith (45 ppi). In these experiments, the reactant gases were preheated to 200°C and the flow rate was 5 slpm.

ratios of 0.6 and 0.75. Propylene and $C_5$ olefins are produced in small amounts from cyclohexane with total selectivities below 0.10.

As in the previous cases, CO is formed selectively at low fuel/$O_2$ ratios while $CO_2$ formation is prevalent at the higher fuel/$O_2$ ratios. Yet for cyclohexane oxidation, $CO_2$ and CO production at the higher fuel/$O_2$ ratios is nearly equal and not dominated by $CO_2$. Also, the formation of oxygenates never increases beyond individual selectivities of 0.03, compared to 0.12 for acetaldehyde in hexane oxidation. In addition, acetylene production is apparent in cyclohexane oxidation, but not in the oxidation of the other fuels.

*Effect of Preheat*

Figures 7 and 8 show the effect of varying the temperature of the feed gases for pentane/air oxidation and cyclohexane/air oxidation respectively. For both fuels, we see that total olefin selectivity remains constant while fuel and $O_2$ conversion increase slightly and then level off with increasing preheat. CO production becomes dominant over $CO_2$ as preheat temperature is raised in both cases.

In pentane/air oxidation, product selectivities change only slightly. Ethylene selectivity increases from 0.31 to 0.33, while propylene and $C_4$ olefin selectivities drop slightly. Fuel conversion increases from 0.62 to 0.72, along with a 100°C increase in catalyst temperature. For cyclohexane oxidation, the olefin selectivities change in a more pronounced fashion while conversion and catalyst temperature remain more constant. Cyclohexene production decreases from 0.18 selectivity to 0.11; butadiene formation increases; and ethylene selectivity increases from 0.15 to 0.20. Fuel and $O_2$ conversion change only slightly, and catalyst temperature increases by less than 50°C despite a 100°C greater change in preheat temperature.

*Reactor Quench*

To determine the extent of any reactions taking place downstream of the monolith catalyst and heat shield, an additional 5 slpm of cold $N_2$ was mixed with the product gases 2 cm from the downstream heat shield. Before quenching, the temperature of the gas in this section of tube was typically 150–200°C below the catalyst surface temperature. After quenching the gas temperature was ~400°C below the catalyst surface temperature (which remained constant before and after quenching). The results of this experiment are shown in Fig. 9.

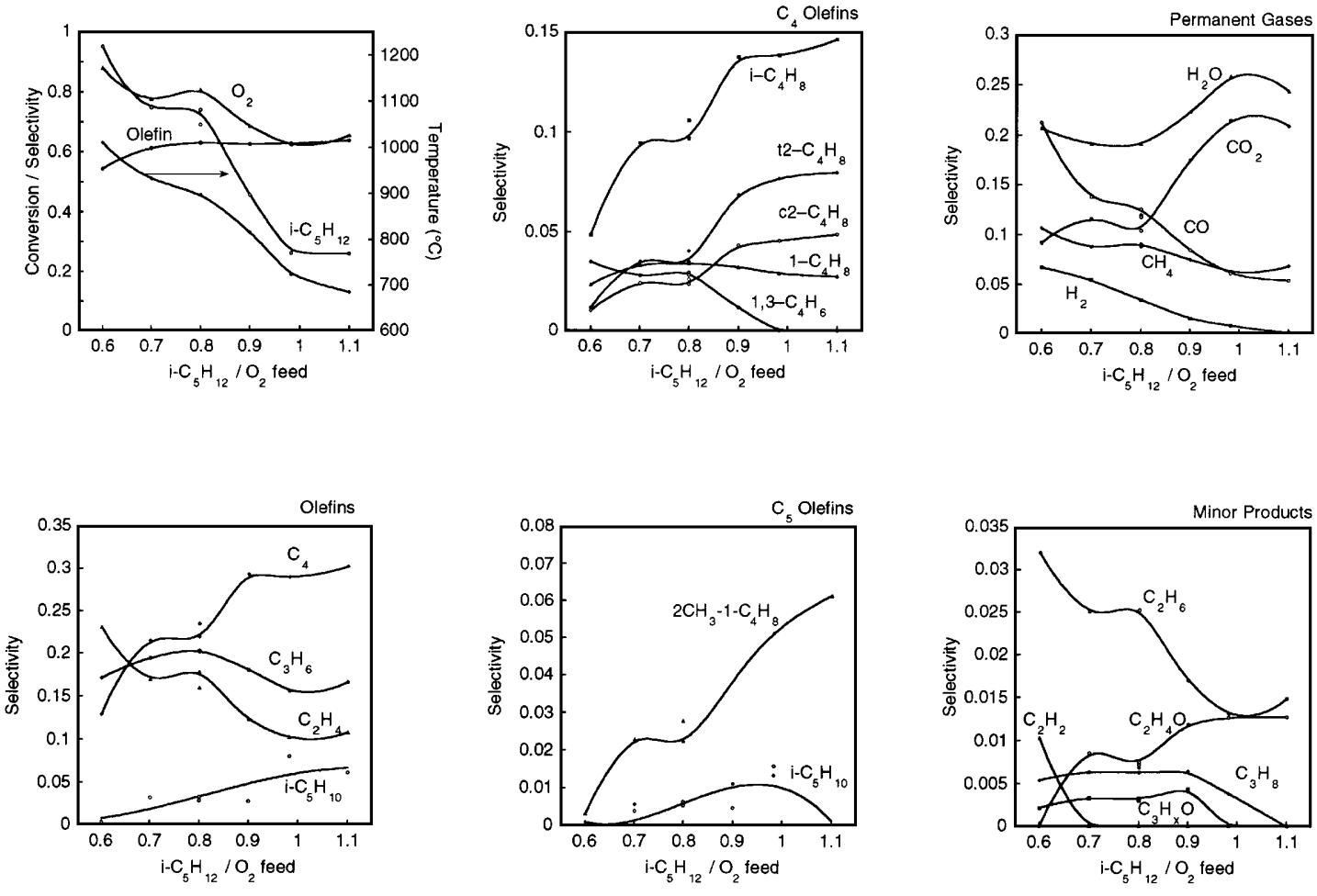


**FIG. 4.** Selectivity and conversion in isopentane oxidation in air versus i-$C_5H_{12}/O_2$ over a Pt coated foam monolith (45 ppi). In these experiments, the reactant gases were preheated to 200°C and the flow rate was 5 slpm.

The selectivity to olefins and to combustion gases are nearly identical to those without reactor quenching. With quenching, conversion of $O_2$ ranges from 0.70 to 0.55, compared to 0.80 to 0.60 without quenching. Conversion of $C_5H_{12}$ ranges from 0.72 to 0.11, compared to 0.85 to 0.33 without reactor quenching. Since the temperature at the surface of the catalyst is identical with and without quenching, some reactions must be taking place in the tube after the catalyst, but this does not strongly affect selectivities.

## DISCUSSION

From these experiments, we observe the following:

(1) Different metals provide quite different product distributions. Partial oxidation of n-pentane over a Rh coated monolith gives primarily CO and $H_2$ over the entire range of fuel/$O_2$ ratios, while over a Pt coated monolith, olefins are the dominant products from n-pentane, and different products dominate at different fuel/$O_2$ ratios. Pd rapidly forms carbon on the catalyst surface and the reaction rapidly extinguishes.

(2) Oxygen conversion is not complete at any fuel/$O_2$ ratios for higher alkanes. Even at low fuel/$O_2$ ratios, some $O_2$ passes through unreacted. When the feed gases are preheated, the $O_2$ conversion increases slightly, but never is complete.

(3) At lower fuel/$O_2$ ratios, cracked olefins are the major products during the partial oxidation of the non-cyclic higher alkanes over Pt coated monoliths. In decreasing order of selectivity, ethylene, propylene, and 1-butene are produced from n-pentane. Isopentane forms isobutylene, propylene, and ethylene. n-Hexane forms primarily ethylene, propylene, and 1-butene. All of which are consistent with $\beta$-scission patterns.

(4) With noncyclic alkanes at higher fuel/$O_2$ ratios, a decrease in the $O_2$ and fuel conversion coincides with a dramatic change in product selectivities and a decrease in the reaction temperature. The selectivities to $CO_2$ and $H_2O$, and oxygenates increase substantially at high fuel/$O_2$

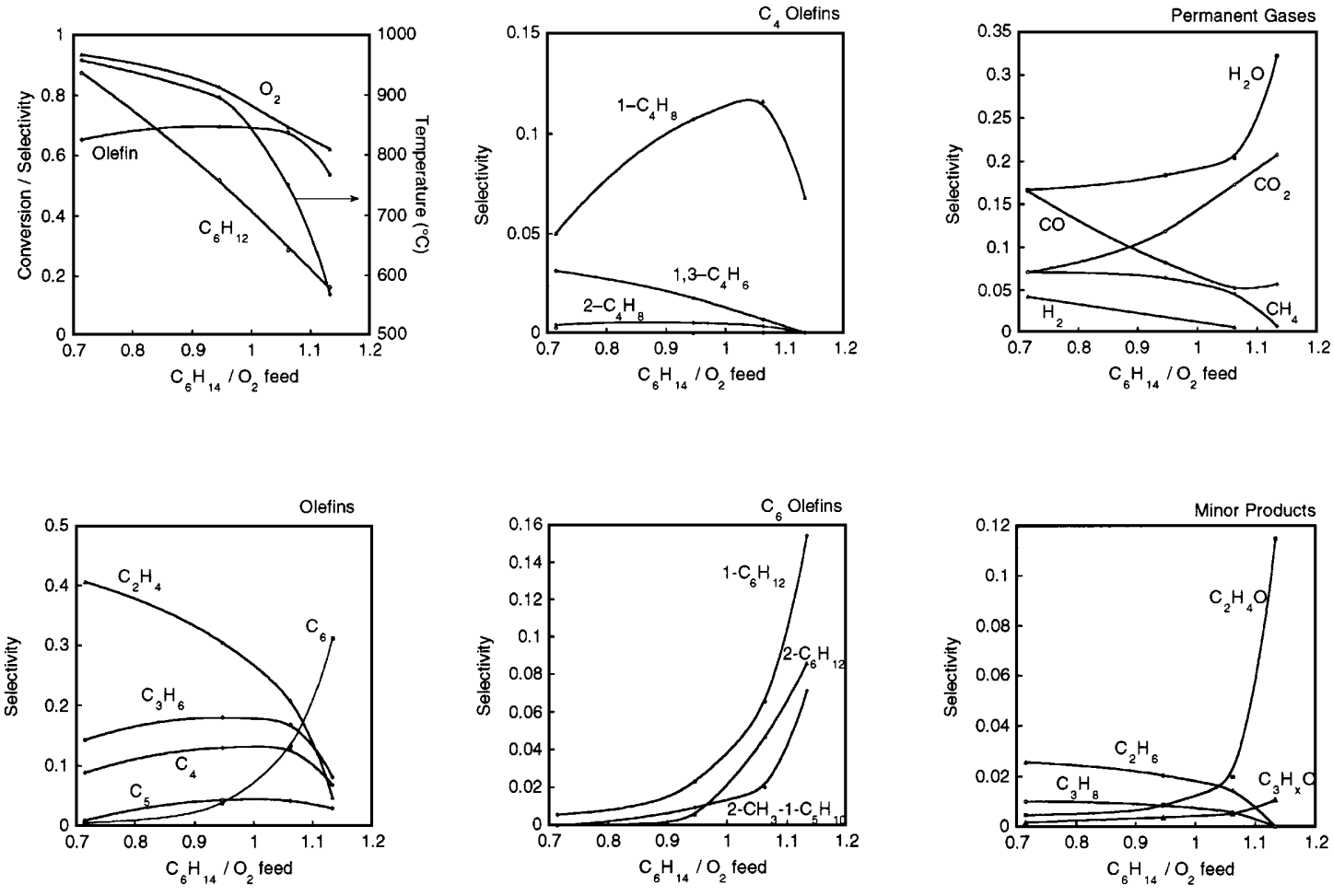


**FIG. 5.** Selectivity and conversion in n-hexane oxidation in air versus $C_6H_{14}/O_2$ over a Pt coated foam monolith (45 ppi). In these experiments, the reactant gases were preheated to 200°C and the flow rate was 5 slpm.

ratios. Olefin production becomes primarily 1-olefins dehydrogenated from the fuel, while CO, $CH_4$, and $H_2$ production all diminish.

(5) Cyclohexane partial oxidation over Pt gives predominantly ethylene and 1,3-butadiene at low fuel/$O_2$ ratios and cyclohexene at high fuel/$O_2$ ratios. Although the CO selectivity decreases, $CO_2$, $H_2O$, and oxygenate selectivities do not change considerably. The temperature of the catalyst for cyclohexane oxidation is ~100°C below that for noncyclic alkane oxidation.

(6) Quenching the reaction with $N_2$ diluent causes reactant conversions to decrease, even though product selectivities do not vary significantly. Whether the downstream reactions are quenched or not, the catalyst temperature is the same.

In the following discussion, we will discuss these observations, paying particular attention to contrasts with previous results on partial oxidation of smaller hydrocarbons over monolith catalysts. We will specifically compare results from the oxidation of the $C_5$–$C_6$ alkanes to results from $C_2$–$C_4$ alkane oxidation. In addition, comparison will be made between product distributions in this work and in thermal pyrolysis. We will also suggest mechanistic routes to the observed products based on surface chemistry, and we will attempt to distinguish the role of homogeneous reactions occurring above the catalyst surface.

### *$C_2$–$C_4$ Partial Oxidation*

A surface mechanism was proposed by Huff *et al.* to explain product selectivities for the oxidation of $C_2$–$C_4$ alkanes (10). On a Pt surface covered with adsorbed O atoms, fuel adsorbs as an alkyl species with an adsorbed O atom, abstracting the fuel H atom to form $OH_s$. To form ethylene from ethane, the $OH_s$ species then abstracts a $\beta$-hydrogen atom from the adsorbed alkyl, which then desorbs to form the olefin. For other adsorbed alkyls, the $\beta$ C–C bond is weaker than the $\beta$ C–H bond, so the $\beta$ C–C bond is preferentially broken to form cracked olefin species. This

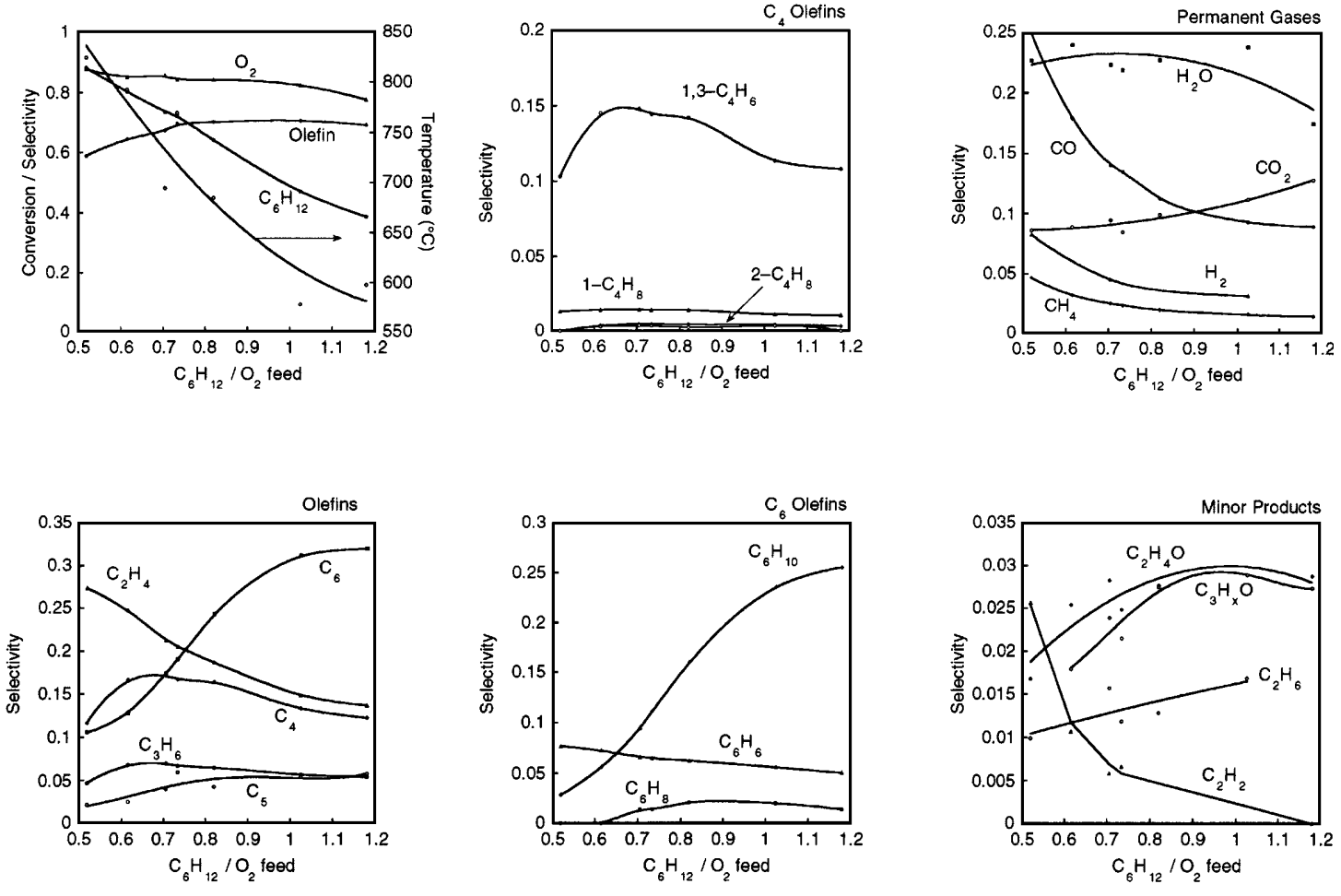


**FIG. 6.** Selectivity and conversion in cyclohexane oxidation in air versus $C_6H_{12}/O_2$ over a Pt coated foam monolith (45 ppi). In these experiments, the reactant gases were preheated to 200°C and the flow rate was 5 slpm.

mechanism can explain some of the olefin product distributions and can explain why five times more isobutylene is formed from isobutane, compared to butene from butane, since isobutane can adsorb such that the only bonds $\beta$ to the adsorbed C are C–H bonds forcing a dehydrogenation reaction to occur (12).

With the higher alkanes, all of the alkyl species that can adsorb have a $\beta$ C–C bond adjacent to the adsorbed C atom. Therefore, cracked products dominate at low fuel/$O_2$ ratios, emphasizing the weakness of the C–C bonds compared to the C–H bonds. With the lower alkanes, often only $\beta$ C–H bonds were available for reaction to form the dehydrogenated olefin as in the case of isobutane oxidation to isobutylene. With the higher alkanes at lower fuel/$O_2$ ratios, the dehydrogenated olefins do not form because there is always a $\beta$ C–C bond to break. Formation of dehydrogenated 1-olefins at high fuel/$O_2$ ratios is explained below.

This $\beta$ elimination mechanism relies on a relatively low activation energy to form $OH_s$ on Pt. On Rh, this activation energy barrier is higher, favoring formation of $H_2$ instead of $OH_s$. This reasoning was used to explain high selectivities to synthesis gas during methane oxidation over Rh monoliths, and it can also explain $H_2$ and CO formation from higher alkanes over Rh (25, 26).

### *Thermal Pyrolysis*

Even though a heterogeneous surface $\beta$-elimination mechanism can explain the products formed in these partial oxidation systems, this does not conclusively eliminate contributions from homogeneous reactions. In Fig. 10, we compare different catalytic oxidation results from lower alkanes to data from thermal pyrolysis of alkanes in long tubular reactors (1, 24). In the thermal pyrolysis reactors, the temperatures (~800°C) were similar to those for partial oxidation, but the contact time was generally ~1 s compared to 5 ms (a factor of 50). In the pyrolysis reactors, steam is added typically at steam/hydrocarbon ratios of 0.4 (kg/kg), but CO and $CO_2$ yields due to reforming are not included in this thermal pyrolysis data. Since $O_2$ is a

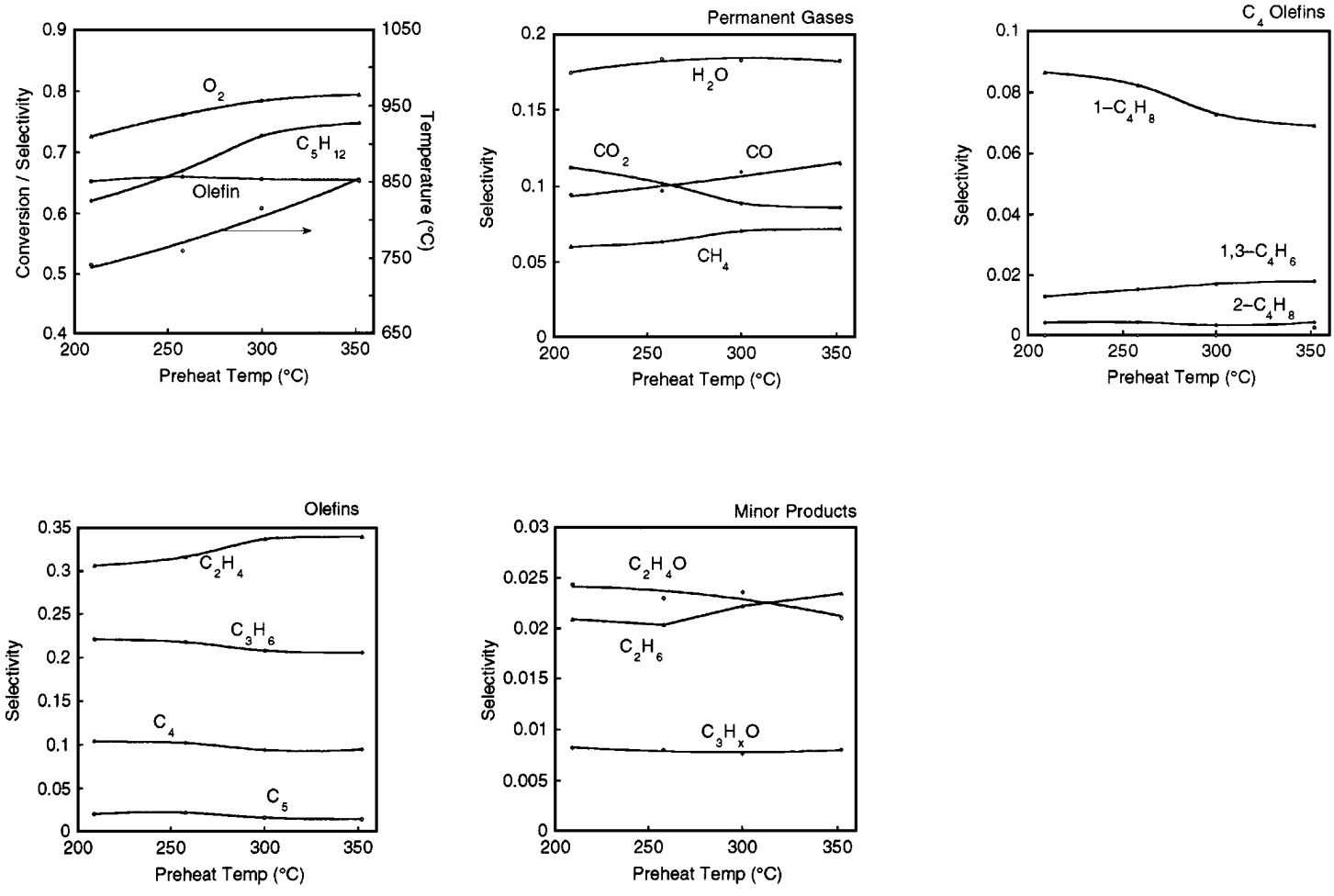


**FIG. 7.** Selectivity and conversion in n-pentane oxidation in air versus preheat temperature over a Pt coated foam monolith (45 ppi). In these experiments, $C_5H_{12}/O_2 = 0.8$ and the flow rate was 5 slpm.

reactant in our systems and is not fed into a steam cracker, we compare C atom selectivities ignoring the formation of CO and $CO_2$ (simply rescaling so a comparison can be made). By eliminating CO and $CO_2$ production, we can extend the comparison to systems such as alkane oxidation over a Rh monolith in which olefins are not the dominant products.

Figure 10 compares the methane and olefin selectivites for ethane, propane, butane, and isobutane catalytic oxidation with typical thermal pyrolysis selectivities at similar fuel conversions (when data is available) (10–12). Catalytic oxidation in air and in oxygen have been included for comparison, as well as ethane and butane oxidation over Rh monoliths, propane oxidation over a gauze catalyst, and isobutane oxidation in a heated empty tube with oxygen. As the bar graphs indicate, the selectivities to olefins for the catalytic oxidation processes are qualitatively similar to those for thermal pyrolysis. The ratios of selectivities are generally preserved for all of the fuels. For example, with n-butane, the $CH_4$ and $C_3H_6$ selectivites are nearly equal, the $C_2H_4$ selectivities are double that, and the $C_4H_8$ selectivites are all small.

Figure 11 shows the dependence of the olefin selectivities (without CO and $CO_2$) on alkane conversion for isobutane catalytic oxidation in air along with the olefin selectivites in thermal pyrolysis. Again, we see that not only are the magnitudes of the selectivities similar, but the trends in the selectivities with respect to isobutane conversion are also preserved. Extending these arguments to higher alkanes is reasonable, but data for thermal pyrolysis is not apparently available since these pure fuels are not generally fed into steam crackers. However, Fig. 12 shows the normalized olefin and alkane selectivities for n-pentane catalytic oxidation over Pt monoliths in air and $O_2$ and over a Rh monolith in air. All of the selectivites for the different systems follow the same trends, and are of the same magnitude.

### *Cyclohexane Oxidation*

Oxidation of cyclohexane shows marked differences from the linear and branched alkanes. In the low fuel/$O_2$

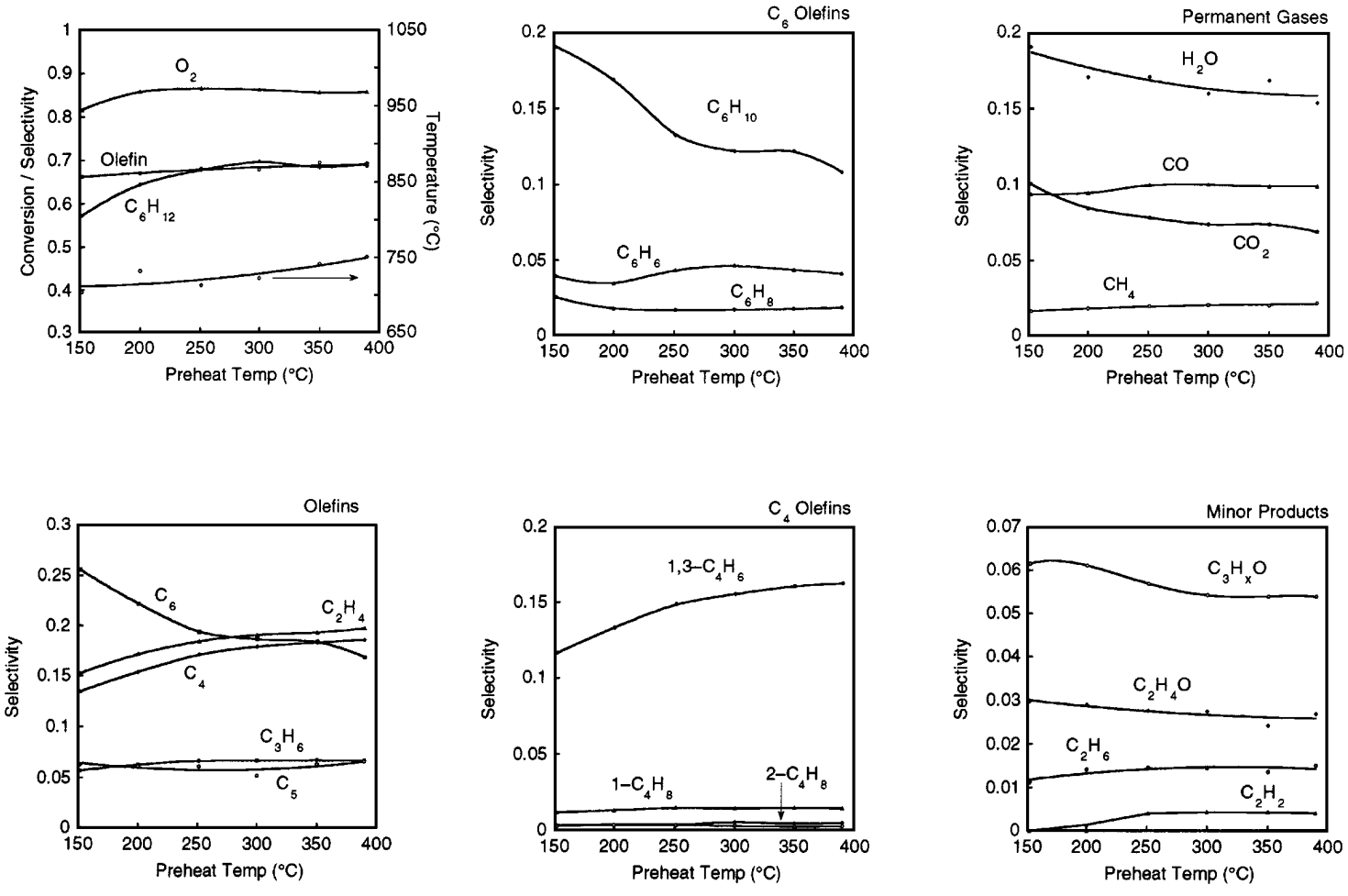


**FIG. 8.** Selectivity and conversion in cyclohexane oxidation in air versus preheat temperature over a Pt coated foam monolith (45 ppi). In these experiments, $C_6H_{12}/O_2 = 0.8$ and the flow rate was 5 slpm.

side of the operating regime, the cyclohexane ring breaks to form ethylene and 1,3-butadiene. Since cyclohexane is already unsaturated, formation of the diene is not surprising. Since only a trace amount of 1,3-butadiene is detected in the noncyclic oxidation compared to mono-olefin production, it is likely that 1,3-butadiene is formed along with ethylene following a ring opening. However, more than 30% of the ethylene production must be accounted from some other reaction pathways.

At low temperatures and pressures, it is accepted that cyclohexane adsorbs on Pt in at multiple bonding sites without C–C bond cleavage, typically as a $\pi$-bonded 1,6 hexadialkylidene species (27–30). Reactions at these conditions produce dehydrogenation to benzene and often to adsorbed $C_s$, with cyclohexene as an intermediate (31). At our experimental conditions, this may explain several of the experimental results. First, the propylene selectivity is small due to the two C–C bonds that are farthest from the surface being very difficult to break with $\beta$-elimination. Second, we see selective formation of cyclohexene along with benzene and cyclohexadiene at high fuel/$O_2$ ratios. As the oxygen coverage on the surface diminishes and fuel coverage rises, abstraction of a $\beta$ hydrogen atom can occur rather than C–C bond cleavage. At low temperatures this would continue to form the cyclohexadiene and benzene, but at higher temperatures desorption can occur to release cyclohexene.

Cyclohexane oxidation over Pt operates about 100°C cooler than for linear and branched alkane oxidation. This can be accounted for by the endothermic ring opening that must occur on cyclohexane to form cracked products, CO, and $CO_2$ which is not required for the non-cyclic alkanes.

### *Carbon Saturation*

With $C_2$–$C_4$ alkanes, oxygen conversion is complete at all operating fuel/$O_2$ ratios. As the carbon chain length increases, $O_2$ conversion decreases, possibly indicating interference by the fuel on catalyst sites that previously contained $O_2$. When the fuel/$O_2$ ratio increases in the oxidation of the noncyclic higher alkanes, the $O_2$ conversion

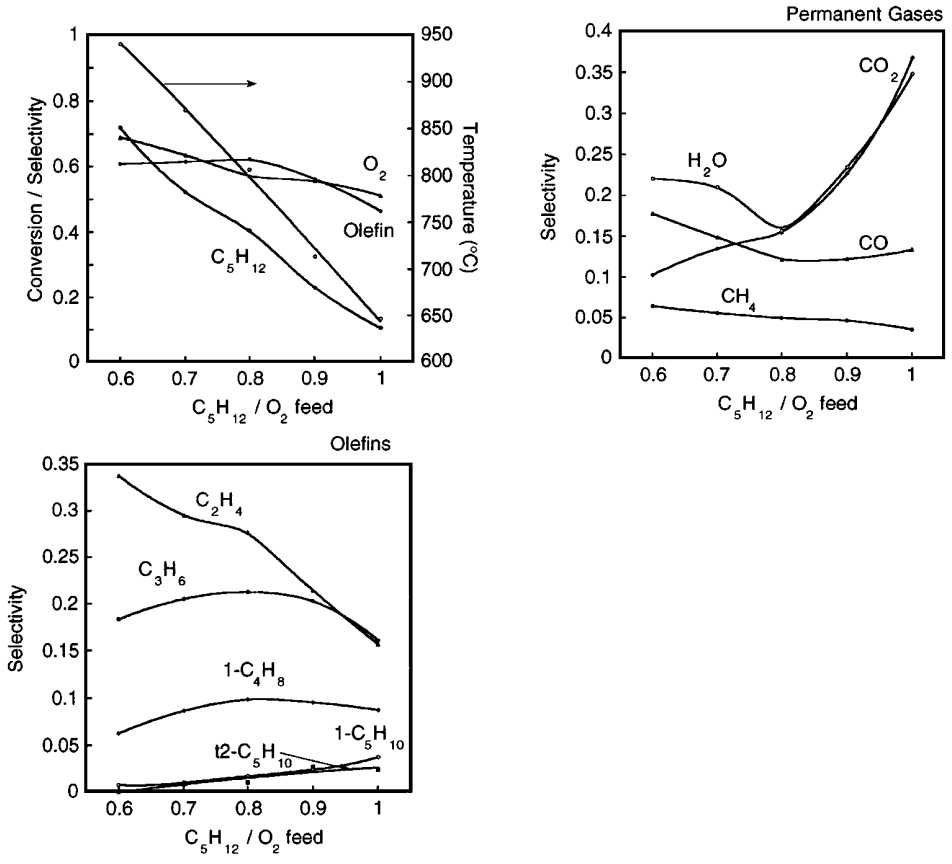


**FIG. 9.** Selectivity and conversion in n-pentane oxidation in air versus $C_5H_{12}/O_2$ over a Pt coated foam monolith (45 ppi) with 5 slpm of $N_2$ quench. In these experiments, the reactant gases were preheated to 200°C and the flow rate over the monolith was 5 slpm.

decreases slightly at first, and then drops off more sharply after C/O > 2. Accompanying the sharp decrease in $O_2$ conversion is a rise in olefins formed from a single alkane dehydrogenation. Among these singly dehydrogenated olefins, 1-olefin production is favored. In contrast, during the oxidation of cyclohexane, $O_2$ conversion decreases slightly but does not exhibit a sharp drop off, although formation of cyclohexene becomes dominant.

In the oxidation of lower alkanes over Pt and Rh monoliths in excess fuel, it was argued that mass transfer of $O_2$ to the surface limits the reaction (26, 32). Once $O_2$ adsorbs as $O_s$ atoms, either an H atom is abstracted from the fuel or oxidation of $C_s$ to CO and $CO_2$ quickly takes place, and $O_2$ conversion is complete. In the systems with higher alkanes, mass transfer rates of $O_2$ should be similar, so the reactions must be inhibited by other factors since $O_2$ conversion is not complete. Larger alkane species may be blocking surface sites that normally would be occupied by adsorbed O atoms. The higher alkanes have higher sticking coefficients than lower alkanes, and they break into many more fragments when cracked. Since hexane can form up to six times more surface carbon than methane, the increased amount of $C_s$ adsorbed to Pt at steady-state operating conditions could cause site blockage. As the fuel/$O_2$ ratio increases, adsorbed alkane and/or $C_s$ concentration should increase, further inhibiting $O_2$ adsorption, perhaps explaining the behavior of $O_2$ conversion with increasing fuel.

Since cyclohexane adsorbs molecularly and then chemisorbs with several of the C atoms away from the surface, linear alkanes adsorbed at the 2 or 3 carbon would lie closer to the Pt surface, becoming more of a steric hindrance than cyclohexane. Therefore, cyclohexane may not inhibit $O_2$ adsorption as much as the higher noncyclic alkanes, resulting in less $O_2$ breakthrough. At high fuel/$O_2$ ratios, there would be more sites available for $O_s$ to help increase $O_2$ conversion. This difference in the Pt surface bond for cyclohexane can also explain why cyclohexene production is dominant, instead of ring opening reactions. If the three carbon atoms away from the adsorbed carbon were closer to the surface, ring opening would be more likely, and cyclohexane chemistry would more resemble that of n-hexane.

When larger amounts of alkanes are adsorbed, steric factors may become important. At lower coverages, the ends of the alkane could swing until the weaker $\beta$ C–C bond came in contact with $OH_s$. If this movement were sterically hindered by high coverage at high fuel/$O_2$ ratios, then the C–H bonds at the ends of the alkane would be attacked by $OH_s$ instead of the C–C bonds, since those are the only bonds

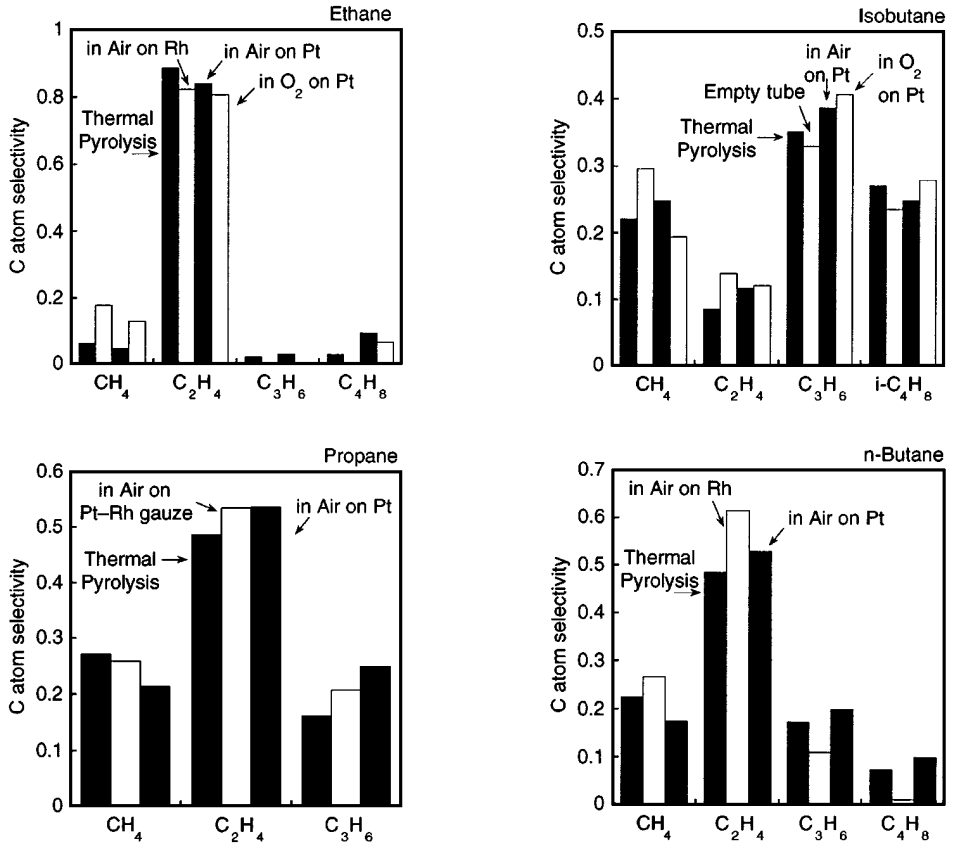


**FIG. 10.** Carbon atom selectivities of olefin products in catalytic oxidation systems and in thermal pyrolysis.

that the $OH_s$ would effectively see. This may explain the selective formation of 1-olefins from the linear and branched alkanes at high fuel/$O_2$ ratios.

*Homogeneous vs Heterogeneous Chemistry*

Figures 10 and 11 indicate that in the catalytic oxidation systems, thermal pyrolysis could be occurring homogeneously after exothermic catalytic reactions to CO, $CO_2$, and $H_2O$. Some major differences do exist between the thermal pyrolysis process and the catalytic oxidation process. First, species residence time in the catalytic process is between 3 and 7 ms, compared to 100 to 1000 ms for steam cracking. Second, no carbon formation is seen in our systems under normal operating conditions. Carbon will form if the section of the tube after the catalyst is insulated, making this section more like a pyrolysis furnace. Third, as Fig. 9 shows, 85% of the $O_2$ and 75% of the fuel that is going to react (based on conversions from Fig. 2) has reacted to form olefins after 12 ms which is much shorter than in typical steam-cracking units. Fourth, significant amounts of coupled and aromatic products are formed in steam cracking that are not detected (<0.1 mol%) in the catalytic oxidations. Even during the catalytic oxidation of the higher linear alkanes, no significant amounts (<0.001 mol%) of coupled or aromatic products were seen.

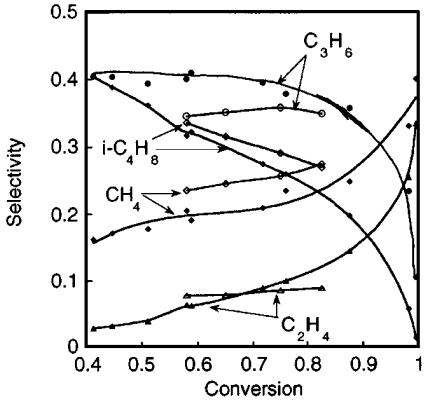


**FIG. 11.** Selectivity in partial oxidation (closed symbols) and thermal pyrolysis (open symbols) versus isobutane conversion.

It is not surprising that similar olefin products are seen in the catalytic oxidation of alkanes and in the steam cracking of alkanes. The product distribution in steam cracking is determined largely by thermodynamic constraints at those temperatures and pressures. In catalytic oxidation, the product distribution is determined by the location of the Pt–C bond and the relative strengths of the C–C and C–H bonds along with thermodynamic driving forces. If

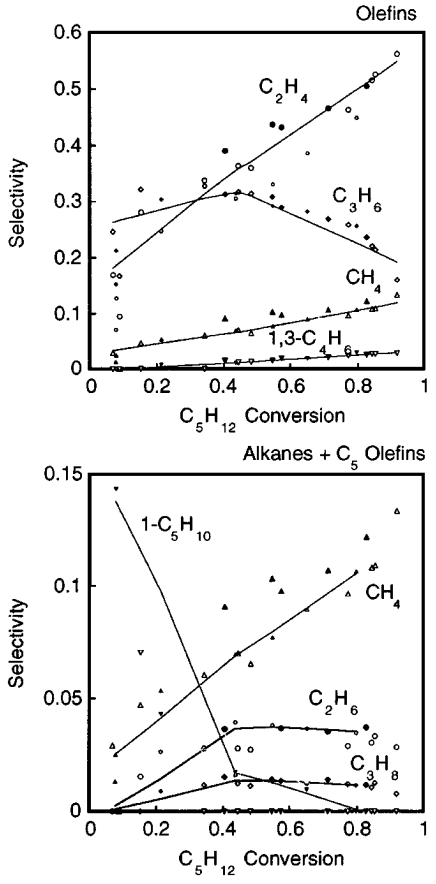


**FIG. 12.** Scaled selectivity versus n-pentane conversion for catalytic oxidation over a Rh monolith (closed symbols), a Pt monolith in air (small open symbols), and a Pt monolith in $O_2$ (large open symbols).

thermodynamics plays a more important role than surface kinetics, then the olefin product distribution would be very similar. In addition, if both the temperature above the catalyst surface and the porosity of the monoliths are high enough not to quench all radical species, then thermal pyrolysis should occur above the catalyst surface, being *catalytically assisted* by oxidation reactions occurring on the metal surface.

Although it may be difficult to determine if the olefinic products at low fuel/$O_2$ ratios are formed homogeneously or heterogeneously, it is more likely that the 1-olefins and cyclohexene are formed heterogeneously by the mechanism described earlier. At high gas temperatures and low $O_2$ conversions, O radicals may form leading to oxygenate production. It is important to note that oxygenate production only becomes significant when $O_2$ conversions are low.

### *Variation of Other Parameters*

In order to determine the roles of homogeneous and heterogeneous chemistry in the partial oxidation of the higher alkanes, other experimental parameters need to be investigated such as the effects of contact time, mass transport, and catalyst geometry.

The effects of contact time on the partial oxidation of lower alkanes over monolith catalysts has been recently examined by Witt *et al.* (33). They conclude that, while production of syngas from methane is detrimentally affected by contact times less than ~1 ms, production of ethylene from ethane is feasible at contact times as short as 200 $\mu$s. Experiments with higher alkanes at short contact times should include quenching experiments in order to determine which reactions are occurring on the catalyst surface and which are occurring above the catalyst surface or downstream of the catalyst. If quenching increases the selectivity to CO and $CO_2$ and causes a drop in conversion, then this points to a homogeneously assisted mechanism for the formation of olefins from alkanes.

Results from the oxidation of methane and butane over Rh catalysts (34) show that very high selectivities to synthesis gas can be achieved with high surface area, high mass transfer catalysts. In the oxidation of the higher alkanes, if a Pt catalysts with more tortuous paths, and thus higher mass transfer, increased selectivities to olefins, this would point to the $\beta$ elimination surface mechanism for olefin production. However, if selectivities to oxidation products (CO + $CO_2$) increased, this would suggest a catalytically assisted mechanism.

Likewise, the addition of Sn-containing species to Pt has been shown to decrease catalyst deactivation and increase selectivity to aromatics (35). Perhaps alloying other metals with Pt would serve to increase conversion and olefin selectivity. The conversion of $O_2$ needs to be nearly complete if a larger scale partial oxidation process with higher hydrocarbons is attempted.

## CONCLUSIONS

We find that olefins can be produced from the catalytic partial oxidation of higher alkanes over Pt coated foam monoliths at very short contact times (~5 ms). The distribution of products is similar to that found in the thermal pyrolysis (steam cracking) of alkanes. This is due to either thermodynamic driving forces to equilibrium after a surface $\beta$ elimination mechanism or a catalytically assisted mechanism by which oxidation reactions to CO, $CO_2$, and $H_2O$ serve to heat the gases above the catalyst, after which steam cracking of the unconverted fuel takes place.

Unlike the catalytic oxidation of lower alkanes on identical monoliths, we see significant oxygen breakthrough at all operating conditions with the higher alkanes. This may be due to fuel species and/or surface carbon blocking $O_2$ from catalytic surface sites. The blockage is more pronounced with the linear and branched higher alkanes, compared to cyclohexane, which may be due to cyclohexane adsorption differences and its propensity to form cyclohexene, instead of cracking and pyrolyzing into surface carbon.

## REFERENCES


1. Albright, L. F., Crynes, B. L., and Cororan, W. H. (Eds.), "Pyrolysis: Theory and Industrial Practice." Academic Press: New York, 1983.
2. Kirk, R. E., and Othemer, D. F. (Eds.), "Encyclopedia of Chemical Technology. Vol. 9. Ethylene." Wiley, New York, 1982.
3. McConnell, C. F., and Head, B. D., Pyrolysis of ethane and propane, *in* "Pyrolysis: Theory and Industrial Practice" (L. F. Albright, B. L. Crynes, and W. H. Corcoran, Eds.), p. 25. Academic Press, New York, 1983.
4. Song, Y., Velenyi, L. J., Leff, A. A., Kliewer, W. R., and Metcalfe, J. E., Steamless pyrolysis of ethane to ethylene, *in* "Novel Production Methods for Ethylene, Light Hydrocarbons, and Aromatics" (L. F. Albright, B. L. Crynes, and S. Nowak, Eds.), p. 319. Dekker, New York, 1992.
5. Ramana Rao, M. V., Plehiers, P. M., and Froment, G. F., *Chem. Eng. Sci.* **43**, 1223 (1988).
6. Froment, G. F., *Chem. Eng. Sci.* **47**, 2163 (1992).
7. Willems, P. A., and Froment, G. F., *Ind. Eng. Chem. Res.* **27**, 1959 (1988).
8. Heynderickx, G. J., Froment, G. F., Broutin, P. S., Busson, C. R., and Weill, J. E., *AIChE J.* **37**, 1354 (1991).
9. Sundaram, K. M., and Froment, G. F., *Ind. Eng. Chem. Fund.* **17**, 174 (1978).
10. Huff, M., and Schmidt, L. D., *J. Phys. Chem.* **97**, 11815 (1993).
11. Huff, M., and Schmidt, L. D., *J. Catal.* **149**, 127 (1994).
12. Huff, M., and Schmidt, L. D., *J. Catal.* **155**, 82 (1995).
13. Dietz III, A. G., and Schmidt, L. D., *Catal. Lett.* **33**, 15 (1995).
14. Huff, M., Torniainen, P. M., and Schmidt, L. D., *Catal. Today* **21**, 113 (1994).
15. Kopinke, F. D., Zimmerman, G., Reyniers, G. C., and Froment, G. F., *Ind. Eng. Chem. Res.* **32**, 56 (1993).
16. Audeh, C. A., and Yan, T. Y., Process of coke formation in delayed coking, *in* "Coke Formation on Metal Surfaces" (L. F. Albright and R. T. K. Baker, Eds.), Vol. 202, p. 295. Am. Chem. Soc., Washington, DC, 1982.
17. Bartholomew, C. H., *Catal. Rev.-Sci. Eng.* **24**, 67 (1982).
18. Heynderickx, G. J., and Froment, G. F., *Ind. Eng. Chem. Res.* **31**, 2080 (1992).
19. Marek, J. C., and Albright, L. F., Formation and removal of coke deposited on stainless steel and vycor surfaces from acetylene and ethylene, *in* "Coke Formation on Metal Surfaces" (L. F. Albright and R. T. K. Baker, Eds.), Vol. 202, p. 123. Am. Chem. Soc., Washington, DC, 1982.
20. Hickman, D. A., and Schmidt, L. D., *J. Catal.* **138**, 267 (1992).
21. Hickman, D. A., Haupfear, E. A., and Schmidt, L. D., *Catal. Lett.* **17**, 223 (1993).
22. Hickman, D. A., Huff, M., and Schmidt, L. D., *Ind. Eng. Chem. Res.* **32**, 809 (1993).
23. Torniainen, P. M., Chu, X., and Schmidt, L. D., *J. Catal.* **146**, 1 (1994).
24. Sundaram, K. M., and Froment, G. F., *Ind. Eng. Chem. Fund.* **17**, 174 (1978).
25. Hickman, D. A., and Schmidt, L. D., *Science* **259**, 343 (1993).
26. Hickman, D. A., and Schmidt, L. D., *AIChE J.* **39**, 1164 (1993).
27. Xu, C., Tsai, Y. L., and Koel, B. E., *J. Phys. Chem.* **98**, 585 (1994).
28. MacPherson, C. D., Hu, D. Q., Doan, M., and Leung, K. T., *Surf. Sci.* **310**, 231 (1994).
29. Tsai, M. C., Friend, C. M., and Muetterties, E. L., *J. Am. Chem. Soc.* **104**, 2539 (1982).
30. Lamont, C. L. A., Borbach, M., Stenzel, W., Conrad, H., and Bradshaw, A. M., *Chem. Phys. Lett.* **230**, 265 (1994).
31. Land, D. P., Pettiette-Hall, C. L., McIver, J. R. T., and Hemminger, J. C., *J. Am. Chem. Soc.* **111**, 5970 (1989).
32. Hickman, D. A., and Schmidt, L. D., *J. Catal.* **136**, 300 (1992).
33. Witt, P. M., and Schmidt, L. D., *J. Catal.* **163**, 465 (1996).
34. Bodke, A., and Schmidt, L. D., unpublished results.
35. Yokoyama, C., Bharadwaj, S. S., and Schmidt, L. D., *Catal. Lett.* **38**, 181 (1996).